ELSEVIER

International Journal of Mass Spectrometry 177 (1998) 119–129

International Journal of Mass Spectrometry

Formation and dissociation of the nitric acid dication

Caroline S.S. O'Connor, Stephen D. Price*

Chemistry Department, University College London, Christopher Ingold Laboratories, 20 Gordon Street, London WC1H 0AJ, UK

Received 5 January 1998; accepted 28 May 1998

Abstract

Electron-impact double ionization of nitric acid, HNO_3 has been investigated by using ion–ion coincidence techniques coupled with time-of-flight mass spectrometry. The coincidence spectra show that HNO_3^{2+} dissociates via a variety of two- and three-body reactions to form the following pairs of ions: $OH^+ + NO^+$, $O^+ + NO^+$, $OH^+ + NO_2^+$, $O^+ + HNO_2^+$, $H^+ + N^+$, $H^+ + O^+$, $H^+ + NO^+$, and $H^+ + NO_2^+$. The experimental data are consistent with the HNO_3^{2+} ion decaying to form the observed ion pairs via an initial charge-separating bond cleavage followed by the dissociation of the resulting singly charged ions. Interpretation of the coincidence spectra yields a determination of the excitation energy required to form the lowest energy dicationic state that dissociates to form $OH^+ + NO_2^+$. Comparison of this excitation energy with estimated values of the double ionization energy of HNO_3 indicate that this state is probably the ground electronic state of HNO_3^{2+} and, hence, these investigations provide a first estimate for the double ionization energy of HNO_3. (Int J Mass Spectrom 177 (1998) 119–129) © 1998 Elsevier Science B.V.

Keywords: Electron ionization; Nitric acid dication; Coincidence spectroscopy; Time-of-flight mass spectrometry

1. Introduction

Nitric acid, HNO_3, is an important trace constituent in the Earth's upper atmosphere and plays a key role in the complex chemistry of the stratospheric ozone cycle. Nitric acid is a reservoir molecule for the nitrogen oxides, NO_x, which are involved in the generation and destruction of ozone and other significant atmospheric effects [1,2]. Despite the atmospheric significance of nitric acid, there have been few investigations [3–5] of the formation and fragmentation of HNO_3^+ and no studies of the double ionization of HNO_3.

The electronic states of doubly charged molecular ions, molecular dications, are commonly thermodynamically unstable, lying at energies above the asymptote for charge separation [6–8]. For many dications, however, metastable states may exist, increasing the lifetime of the dication to the order of the mass spectrometric time scale or longer [9–11]. Over recent years, the properties of dications have been extensively reviewed in the literature and have also been the subject of a steadily increasing number of experimental investigations, due in part to the development of several new techniques to probe these short-lived species [6–8]. As a result of these experimental efforts, an increasing amount of information has been obtained concerning the energetics and dissociation mechanisms of the low-lying electronic states of several diatomic and triatomic dications,

* Corresponding author.

PII S1387-3806(98)14056-3

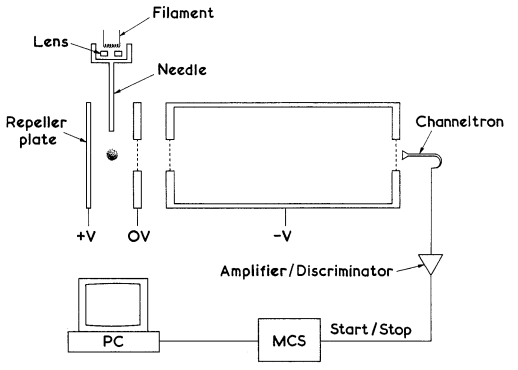

Fig. 1. Schematic diagram of the time-of-flight mass spectrometer. The gas inlet, which is perpendicular to the plane of the figure, is not shown.

including energies and dissociation dynamics of the vibrational levels in dication metastable electronic states [12–15].

As part of an ongoing investigation of the ionization of reactive species, and following a successful study of the single ionization of HNO_3 [5], this article reports an investigation of the formation and fragmentation of the HNO_3 molecular dication using ion–ion coincidence techniques [16]. Comparison of the experimentally determined appearance energies for the dissociation reactions of HNO_3^{2+} with the energetics derived from the kinetic energy release (KER) involved in these dication dissociation processes can give an indication of the mechanisms by which HNO_3^{2+} dissociates and the energy of the dication electronic state that are the source of the fragment ions.

2. Experimental

The apparatus used for these experiments is a conventional time-of-flight mass spectrometer (TOFMS) of the standard Wiley–McLaren design [17]. This apparatus is illustrated schematically in Fig. 1 and a detailed description of it has been presented in previous publications [18,19]. In brief, ionization occurs in the source region of the TOFMS, at the intersection of an effusive jet of target molecules with an electron beam. The ions formed following the interaction of the electron beam with the target gas are accelerated into the drift region of the TOFMS and finally impinge on a channeltron multiplier. Time-of-flight mass spectra can be recorded on this apparatus by pulsing the source electric field on and off and recording the subsequent ion arrival times in a multichannel scalar [18]. Since using conventional time-of-flight mass spectrometry it is difficult to distinguish definitively between the monocation fragments generated by the dissociation of HNO_3^+ and those resulting from the dissociation of the HNO_3 dication, in this work ion–ion coincidence experiments [16,18–22] have been performed to detect and identify the pairs of ions produced by dissociative double ionization of HNO_3. For these ion–ion coincidence experiments, the electric field across the source region is no longer pulsed but applied continuously. This field immediately accelerates any ions formed towards the detector. Coincidence spectra are recorded by measuring the time-of-flight difference between the arrival times at the detector of pairs of fragment ions formed following the rapid charge-separating dissociation of a molecular dication. The experimental procedure has been described extensively in previous publications [18,19] and will therefore not be discussed here.

The nitric acid sample used for these experiments was prepared by the removal of the water from a commercially purchased sample of nitric acid (HNO_3 content $>$90%) by repeated vacuum distillation over P_2O_5. During the experiments the anhydrous liquid acid was placed in a salted ice bath, at a temperature of approximately 255 K. The gaseous sample is transported into the ionization region of the TOFMS by using a clean and noncatalytic glass/Teflon inlet system [23]. Typical operating pressures in the TOFMS were of the order of 6×10^{-5} Pa, as recorded by an ion gauge. Low operating pressures are required to ensure a good signal-to-noise ratio in coincidence experiments [19].

Coincidence spectra of HNO_3^{2+} were recorded at an ionizing electron energy of 150 eV and also at a range of lower electron energies from 30–70 eV in order to determine the appearance energies of the pairs of fragment ions produced by the dissociative double ionization of HNO_3. The electron energy

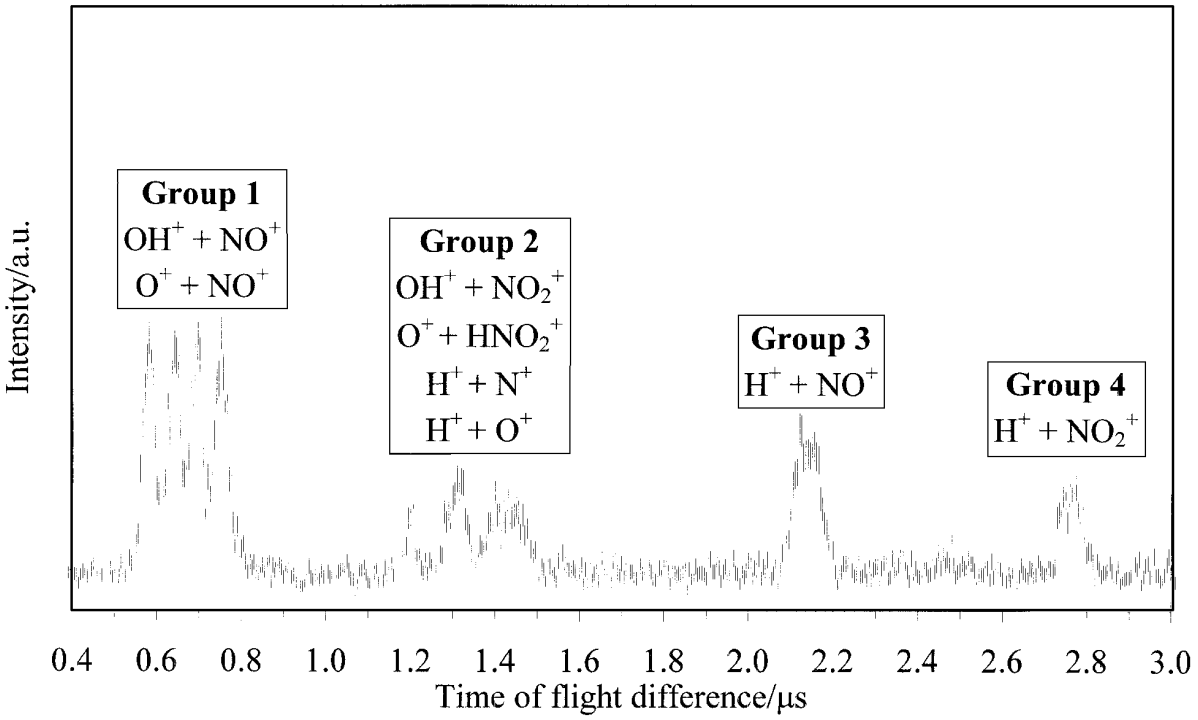

Fig. 2. Ion–ion coincidence spectrum of HNO_3^{2+}, generated by electron impact at 150 eV. The error bars shown are of length 2σ, where σ is derived from the counting statistics. As explained in the text, the coincidence peaks have been separated into four distinct groups.

resolution has been conservatively estimated by previous experiments to be ±2 eV [23].

3. Data analysis

A typical ion–ion coincidence spectrum of HNO_3^{2+} recorded on our apparatus is shown in Fig. 2. The dissociation reactions observed are listed below and, as indicated, have been separated in four distinct groups, for ease of analysis:

Group 1 $HNO_3^{2+} \rightarrow OH^+ + NO^+ [+O]$ (1)

$HNO_3^{2+} \rightarrow O^+ + NO^+ [+H + O]$ (2)

Group 2 $HNO_3^{2+} \rightarrow OH^+ + NO_2^+$ (3)

$HNO_3^{2+} \rightarrow O^+ + HNO_2^+$ (4)

$HNO_3^{2+} \rightarrow H^+ + N^+ [+3O]$ (5)

$HNO_3^{2+} \rightarrow H^+ + O^+ [+N + 2O]$ (6)

Group 3 $HNO_3^{2+} \rightarrow H^+ + NO^+ [+2O]$ (7)

Group 4 $HNO_3^{2+} \rightarrow H^+ + NO_2^+ [+O]$ (8)

The neutrals are listed in parentheses as they are not detected, but, as described below, they are most likely to be completely fragmented. As can be seen from Fig. 2, there is a great deal of congestion in certain regions of the coincidence spectrum and upon initial inspection it is not possible to discern definitively which dissociation reactions contribute to the coincidence signal in these regions. However, as explained below, a computer simulation of the experimental data enables the identification of all the dissociation reactions present. Any coincidence signals produced by the formation of identical fragment ions cannot be efficiently detected in our coincidence apparatus [19] and were therefore not investigated further. Pairs of similar mass ions, e.g. $N^+ + O^+$, can be detected by using this experimental setup [19], but we saw no evidence for the presence of such pairs in our spec-

trum. The spectrum also contains very weak signals resulting from the double ionization of water, the principal background gas in the apparatus.

The shape of the coincidence peaks, Fig. 2, arises because of the experimental angular constraint imposed by the small entrance aperture of the channeltron, resulting in the selective detection of pairs of fragment ions formed from dissociation events where the KER is directed principally along the axis of the TOFMS [19].

The KER associated with the formation of an ion pair from dicationic dissociation is related to the temporal width of the coincidence peak [19]. If the KER can be determined for a given fragmentation channel, then an estimate of the energy of the dication state from which the decay reaction occurred can be made by adding the KER to the energy of the products of the charge separation reaction. As described in a previous publication [19], a Monte-Carlo simulation [16,24,25] of the coincidence spectrum is used to obtain a determination of the KER and the corresponding half-width of the KER distribution F_{KERD} associated with a given dication fragmentation channel. Repeated simulations of the coincidence spectrum are performed until a satisfactory fit with the experimental data is obtained. The uncertainties in the KER and F_{KERD} derived from such a fit, determined by the deviations necessary to significantly degrade the fit with the experimental spectrum, are of the order of ± 0.2 eV. It has been shown in previous work that this analysis procedure provides reliable KER and F_{KERD} values [16,19,26].

Figure 3 shows the comparison of a simulated spectrum with typical experimental data recorded at an ionizing electron energy of 150 eV. Due to the extensive overlapping of signals in this region of the coincidence spectrum (Fig. 3), it is difficult to identify by eye any weak signals that may be present. However, by using the simulation procedure it is possible to determine which ion pairs are contributing to the coincidence signal in a particular region of the spectrum by comparing the fit of the simulated spectrum with the experimental data. Indeed, upon inclusion of the weak signals corresponding to $H^+ + N^+$ and $O^+ + HNO_2^+$ in the simulation procedure the fit with the experimental spectrum is markedly improved, providing good evidence that these dissociation reactions of HNO_3^{2+} do indeed occur. However, as the signals for the $H^+ + N^+$ and $O^+ + HNO_2^+$ ion pairs are very weak and overlapped by the more intense signals of $OH^+ + NO_2^+$ and $H^+ + O^+$, it is very difficult to derive reliably the KER associated with these minority dissociation reactions.

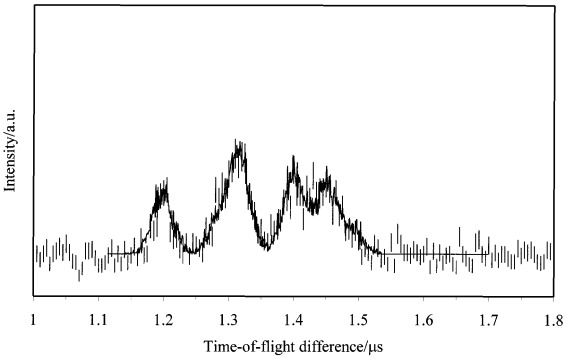

Fig. 3. Ion–ion coincidence spectrum showing the peak corresponding to group 2 contains the $OH^+ + NO_2^+$, $H^+ + N^+$, $O^+ + HNO_2^+$, and $H^+ + O^+$ ion pairs. The experimental points are indicated by error bars of length 2σ. The solid curve is a Monte-Carlo simulation of the experimental signal including all four of the dissociation reactions in the ratio 8.6:4.2:1:6.2.

The ion pairs observed in the coincidence spectrum are formed by both two- and three-body dissociation reactions of HNO_3^{2+}. There is only one possible decay pathway for a two-body dissociation reaction: the direct dissociation of the molecular dication to form the two product ions [Eqs. (3) and (4)]. Whereas the three-body reactions, where neutral products are formed in addition to the pair of fragment ions [Eqs. (1), (2), and (5)–(8)], can occur via three general pathways [27]. The first pathway involves the direct dissociation of the dication to form the two ions and neutrals, a Coulomb explosion. The second and third pathways are both sequential mechanisms involving either a deferred charge separation or an initial charge separation that is then followed by the dissociation of one or more of the resulting ions to form the detected pair of singly charged ions. So, for a three-body dissociation reaction, the pair of ions detected in the coincidence spectrum may not be the same two ions that received the initial impulse from the dicationic

dissociation event. As a result, the interpretation of the widths of the coincidence peaks, in terms of the KER upon dissociation, is complicated and in order to make further progress in understanding the dissociation of HNO_3^{2+}, one must consider the three-body fragmentation pathways by which the dication dissociates.

As described above, the KER associated with the temporal width of the coincidence peak depends on the masses of the pairs of ions formed in the initial charge separation. For the two-body reactions, the dicationic dissociation mechanism to form these ion pairs is unambiguous. Therefore, the result of the simulation procedure for a two-body reaction is a single value of the KER and corresponding F_{KERD}.

For the three-body dissociation reactions, the primary ions formed by charge separation of the dication are not necessarily the ones detected in the coincidence spectrum. However, triple coincidence studies of the dissociation reactions of small polyatomic dications [27–32] have shown that a true Coulomb explosion is rare. They have also shown that if daughter dications are not observed in the mass spectrum [5] and there are no metastable tails on the coincidence signals, implying the existence of a long-lived daughter dication, as is the case here, the dissociation mechanism is unlikely to involve deferred charge separation. Therefore, we can make further progress analyzing the peak shapes in the coincidence spectrum if we assume that the mechanism by which the three-body dissociation reactions of HNO_3^{2+} occur involves an initial two-body charge separation followed by the dissociation of one or more of the resulting singly charged ions to form the detected ion pairs.

We have performed the simulation procedure for the three-body reactions several times, modeling the formation of the detected ion pairs via all the possible initial two-body charge separations and subsequent singly charged ion dissociation pathways. In this process we assume that the KER of the monocation dissociation is negligible in comparison to the primary KER of the dication dissociation. The result of the simulation procedure for the three-body reactions is a list of the potential KER and F_{KERD} values required to fit the simulated spectrum to the experimental data for each dissociation reaction. For example, Table 1 shows the potential KER and F_{KERD} values for the possible dissociation reactions forming the $H^+ + NO_2^+$ ion pair.

Table 1
Potential values of the kinetic energy release KER, half-width of the kinetic energy release distribution F_{KERD}, and dication state energy $E(HNO_3^{2+})$ for the dissociation reaction in group 4, forming the $H^+ + NO_2^+$ ion pair, derived by simulation of the ion–ion coincidence spectrum at 150 eV. As shown in the table, and described in the text, the KER and F_{KERD} values are dependent on which pathway the dissociation of HNO_3^{2+} to form $H^+ + NO_2^+$ is assumed to follow

Initial charge separation	KER /eV	F_{KERD} /eV	Potential $E(HNO_3^{2+})$ /eV
$OH^+ + NO_2^+$	2.3	0.5	32.2
$H^+ + NO_3^+$	8.0	1.0	37.9

For each three-body reaction, the KER value that is correct depends upon the pathway by which HNO_3^{2+} fragments to form the relevant ion pair. So, in order to derive some mechanistic information from these potential KER values, it is necessary to determine experimentally the threshold (appearance energy) of each dication fragmentation pathway and compare it with the energy of the dication state responsible for the dissociation, calculated by using the potential KER values derived from the simulation procedure. Such comparisons can give an indication of the dicationic decay pathway followed to form the relevant ion pair. This analysis procedure has proved successful in a previous study of the formation and dissociation of $N_2O_5^{2+}$ [19].

The appearance energies of the signals making up groups 1, 3, and 4 have been determined by monitoring the yield of each group of reactions with respect to the ion count rate, as a function of electron energy. In congested areas of the coincidence spectrum the appearance energy of each individual dissociation reaction cannot be determined separately due to the extensive overlapping of the coincidence signals that are impossible to deconvolute near threshold where the double ionization cross section is small. As explained in greater detail previously [18,19], as the ionizing electron energy approaches threshold, the

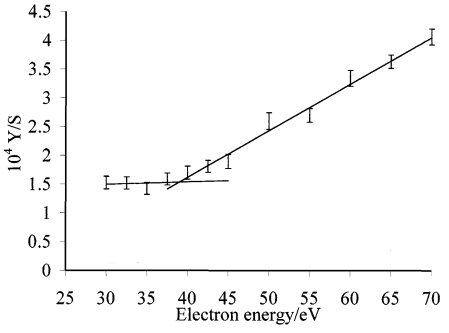

Fig. 4. A plot of the ion yield (Y) of the dication dissociation reaction to the number of coincidence starts (S) as a function of electron energy for group 1, containing the $OH^+ + NO^+$ and $O^+ + NO^+$ ion pairs. As described in the text and illustrated in the figure, the plot can be interpreted to yield the ionization threshold of the lowest energy dication state responsible for the decay reactions forming the $OH^+ + NO^+$ and $O^+ + NO^+$ ion pairs.

ratio of the yield Y of a decay reaction, or group of reactions, to the number of coincidence starts S is proportional to σ_2/σ_1, where σ_1 and σ_2 are the single and double ionization cross sections, respectively. Thus, a plot of Y/S against electron energy should fall to zero at the energy of the lowest-lying dictation state contributing to the relevant decay reactions, the threshold for the formation of the particular group of ion pairs.

The ratio Y/S was carefully evaluated for groups 1, 3, and 4 at electron energies from 30 to 70 eV. Figure 4 shows a weighted least-squares fit applied to the values of Y/S for group 1 above and below the threshold. Group 1 contains the ion pairs $OH^+ + NO^+$ and $O^+ + NO^+$ and the signals corresponding to both ion pairs are observed at electron energies close to threshold. Y/S can be extrapolated to the non-zero background level of residual double ionization [19] and a value of 39.0 ± 2 eV is obtained for the threshold of group 1. The errors associated with this determination of the threshold are evaluated by considering the energy resolution of the ionizing electron beam.

The values of Y/S as a function of electron energy, evaluated by using the same method, are listed in Table 2 for groups 3 and 4. At low electron energies the statistical (counting) uncertainties in Y/S are significantly increased for these weaker signals and the evaluation of their thresholds is subject to a greater uncertainty. The threshold for group 2 was not determined as the uncertainties in Y/S were so large as to make an evaluation of the threshold impractical.

Table 2
Values of the ratio of the ion yield (Y) of the dication dissociation reactions making up groups 3 and 4 to the number of coincidence starts (S) as a function of electron energy. As described in the text, these values can be interpreted to yield an ionization threshold associated with each group. The numbers in parentheses indicate the standard deviation in the last figure of each Y/S value

Electron energy/eV	10^4 Y/S	
	Group 3	Group 4
30.0	0.150 (71)	0.142 (61)
32.5	0.237 (70)	0.053 (59)
35.0	0.226 (65)	0.115 (55)
37.5	0.160 (66)	0.192 (57)
40.0	0.130 (74)	0.040 (63)
42.5	0.139 (67)	0.053 (57)
45.0	0.270 (77)	0.289 (66)
50.0	0.454 (92)	0.267 (79)
55.0	0.486 (74)	0.368 (64)
60.0	0.593 (87)	0.316 (74)
65.0	0.558 (75)	0.425 (64)
70.0	0.801 (87)	0.440 (74)

The KERs derived from the simulation procedure are transformed into values of the dication state energy, $E(HNO_3^{2+})$, by using the following equation:

$$E(HNO_3^{2+}) = E_{ASYM} + \text{KER} \quad (9)$$

where E_{ASYM} is the energy of the dissociation asymptote for forming the relevant products in their ground states and can be derived from thermodynamic tables [33]. In the calculation of $E(HNO_3^{2+})$, the fragment ions and neutral atoms are assumed to be formed with no internal energy and previous studies have shown that this is usually a valid approximation [16]. Therefore, any value of $E(HNO_3^{2+})$ derived in this way should really be considered a lower limit. Because there is a only one possible decay pathway for a two-body dissociation reaction, the unambiguous KER derived from the coincidence peak widths is converted into a single value of $E(HNO_3^{2+})$ for each two-body reaction. From the potential KER values for the three-body reactions, corresponding potential

Table 3
Potential values of the kinetic energy release KER, half-width of the kinetic energy release distribution F_{KERD}, and dication state energy $E(HNO_3^{2+})$ for the dissociation reaction in group 3, forming the $H^+ + NO^+$ ion pair, derived by simulation of the ion–ion coincidence spectrum at 150 eV. As shown in the table, and described in the text, the KER and F_{KERD} values are dependent on which pathway the dissociation of HNO_3^{2+} to form $H^+ + NO^+$ is assumed to follow and the form of the neutral products

Initial charge separation	KER/eV	F_{KERD} /eV	Potential $E(HNO_3^{2+})$ /eV	
			[+2O]	[+O_2]
$OH^+ + NO_2^+$	6.5	5.0	39.1	···
$H^+ + NO_3^+$	10.6	7.0	43.2	36.1

$E(HNO_3^{2+})$ values are obtained (see Table 3, for example, for such values for the $H^+ + NO^+$ ion pair). As illustrated in Table 3, the value of $E(HNO_3^{2+})$ depends not only on the initial two-body charge-separating dissociation reaction, but also on the form of the neutral products. These potential values of $E(HNO_3^{2+})$ can then be compared with the experimentally determined thresholds. If, for a given dication three-body fragmentation channel, unambiguous agreement is found between one value of $E(HNO_3^{2+})$ derived from the simulation procedure and the experimentally determined threshold, then this provides good evidence that the mechanism used to derive the KER is the one that is actually followed to form the detected ion pairs [19].

4. Discussion

Our coincidence spectra show that the molecular dication HNO_3^{2+} dissociates via a variety of two- and three-body reactions. In the electron-impact mass spectrum of HNO_3 [3,5] no stable parent dication (HNO_3^{2+}) or daughter dications are observed. This implies that any bound regions of the dication potential energy surfaces cannot be accessed by a vertical transition from the equilibrium geometry of the neutral molecule. As explained above, the coincidence signals in the spectrum have been separated into four distinct groups for ease of analysis.

4.1. Group 1: $OH^+ + NO^+$ and $O^+ + NO^+$

The coincidence signals making up group 1 (Fig. 2) lie between a time-of-flight difference of 0.5 and 0.8 μs in the coincidence spectrum. The experimentally determined threshold for this group (Fig. 4) is 39.0 ± 2 eV. This value could be interpreted as the energy of the lowest-lying dication state responsible for forming either the $OH^+ + NO^+$ or $O^+ + NO^+$ ion pairs. However, the appearance energy appears to be the same for both ion pairs as signals corresponding to both ion pairs are observed right down to threshold. Therefore, we consider that these dissociation reactions probably occur from the same electronic state of the dication that lies at 39.0 ± 2 eV.

Interpretation of the coincidence signals from HNO_3^{2+} forming the $OH^+ + NO^+$ ion pair, assuming the obvious initial two-body charge separation to $OH^+ + NO_2^+$, yields a value of $E(HNO_3^{2+})$ of 35.3 eV, which is considerably lower than the experimentally determined threshold.

For the three-body dissociation reaction forming the $O^+ + NO^+$ pair, the possible decay pathways involve initial two-body fragmentation to form $OH^+ + NO_2^+$ and $O^+ + HNO_2^+$ which yield values of $E(HNO_3^{2+})$ as 39.6 and 39.7 eV, respectively. Note that both these initial two-body reactions are also observed in the coincidence spectrum, the intensity of the $OH^+ + NO_2^+$ signal being far greater than that of the $O^+ + HNO_2^+$ signal.

As the threshold appears to be the same for both $OH^+ + NO^+$ and $O^+ + NO^+$, we believe it is possible that the dissociation of HNO_3^{2+} to form these ion pairs occurs from the same dicationic electronic state. If this is indeed the case, then the formation of both ion pairs might arise from the same initial two-body charge-separating reaction: $OH^+ + NO_2^+$. The alternative pathway involving an initial fragmentation to $O^+ + HNO_2^+$ is considered less likely as the ion pair $OH^+ + NO^+$ could not be formed from this initial charge separation. Therefore, the most consistent interpretation of our experimental data is that the initial two-body dissociation for both reactions is a charge-separating reaction to $OH^+ + NO_2^+$. In this interpretation these primary monocations must have

the opportunity to be formed with some internal excitation and can therefore undergo subsequent dissociation reactions to form the two ion pairs observed in this group, first $OH^+ + NO^+$ and after further dissociation $O^+ + NO^+$ [Eq. (10)].

$$\begin{array}{lcccl} HNO_3^{2+} \rightarrow & OH^{+*} & + & NO_2^{+*} & \\ & \downarrow & & \downarrow & \\ & OH^{+*} & + & NO^+ + O & (10) \\ & \downarrow & & \downarrow & \\ & O^+ & + & NO^+ + H + O & \end{array}$$

Assuming that the mechanism shown in Eq. (10) is the pathway by which HNO_3^{2+} dissociates to form $OH^+ + NO^+$ and $O^+ + NO^+$, the relevant values of $E(HNO_3^{2+})$ for these two dissociation reactions are 35.3 and 39.6 eV. The value of 39.6 eV derived for the $O^+ + NO^+$ reaction is an excellent agreement with the experimentally determined threshold. However, the value of $E(HNO_3^{2+})$ derived for the $OH^+ + NO^+$ reaction (35.3 eV) is markedly lower than the threshold. But, this value is expected to be too low as it does not allow for the internal excitation in the OH^+ ion that we consider must be present [Eq. (10)]. Indeed, if some of the OH^+ ions fragment to O^+ they must possess at least 5.1 eV of internal energy [33]. Hence, if this mechanism is indeed followed it is reasonable that the OH^+ ions detected together with NO^+ possess several electron volts of internal excitation. Therefore, given these considerations the two values of $E(HNO_3^{2+})$, 35.3 and 39.6 eV, derived from the coincidence spectra are consistent.

4.2. Group 2: $OH^+ + NO_2^+$, $H^+ + N^+$, $O^+ + HNO_2^+$, and $H^+ + O^+$

The coincidence peaks making up group 2 (Fig. 2) are in the region of the coincidence spectrum at a time-of-flight difference from 1.1 to 1.6 μs. An accurate evaluation of the experimentally determined threshold for this group is difficult to obtain as the signal is very weak at low electron energies and there are a large number of contributing dissociation reactions that cannot be accurately resolved given the low double ionization cross section at low electron energies. By using the simulation procedure described above, the values of the KER and the associated $E(HNO_3^{2+})$ derived for a sequential decay pathway involving an initial two-body charge separation were determined for the reactions in this group.

As mentioned above, there are no mechanistic complications associated with two-body dissociation reactions as there is only a single possible decay pathway. The energy of the dication state responsible for the two-body decay reaction forming $OH^+ + NO_2^+$ was found to be 30.7 ± 0.2 eV. The signal corresponding to the second two-body reaction forming $O^+ + HNO_2^+$ is very weak indeed and occurs in a region of the coincidence spectrum where there is extensive overlapping of the coincidence signals. Therefore, it is impossible to derive a value for the KER associated with this decay reaction. Given this lack of information on the $O^+ + HNO_2^+$ dissociation, it is not possible to discern if the pair of two-body dissociation reactions occur as a result of the population of two distinct electronic states of the dication or the population of the same dicationic electronic state. The fair agreement between the value of the $E(HNO_3^{2+})$ obtained for $OH^+ + NO_2^+$ (30.7 eV) and an estimate of the double ionization potential as 33.5 eV, generally considered accurate to within ±10%, obtained by using the "rule of thumb" [34], indicates that this two-body dissociation reaction probably occurs from the ground electronic state of HNO_3^{2+}. Therefore our coincidence spectra place a lower limit on the double ionization energy of nitric acid as 30.7 eV.

The signal corresponding to the $H^+ + N^+$ pair is also very weak indeed and occurs in a congested region of the coincidence spectrum. As a result, it is impossible to derive a precise value of the KER and $E(HNO_3^{2+})$ associated with this decay reaction. More detailed analysis of the energetics and associated mechanism to form the $H^+ + O^+$ ion pair is also difficult as there are a number of possible dication dissociation pathways, but the lack of an experimentally determined threshold for comparison with any calculated values of $E(HNO_3^{2+})$ means no definitive dissociation mechanism can be assigned.

4.3. Group 3: $H^+ + NO^+$

The coincidence signal corresponding to $H^+ + NO^+$ (Fig. 2) lies between a time-of-flight difference of 2.05 and 2.25 μs in the coincidence spectrum. Again, the appearance energy of this dissociation reaction could not be determined to our usual accuracy ($\pm$2 eV) due to the weak signal at low electron energies. The threshold is found to be 40 $\pm$ 5 eV (Table 2). As can be seen from Table 3, there are two possible initial two-body fragmentations that, after further dissociation, could result in the formation of the $H^+ + NO^+$ ion pair. As shown in Table 3, the values of the KER and F_{KERD}, derived assuming the formation of the $H^+ + NO^+$ ion pair via initial charge separation to $H^+ + NO_3^+$, are unrealistically large for the dissociation of a polyatomic dication. Therefore, we consider this decay pathway is unlikely to be responsible for the dissociation reaction. The remaining fragmentation pathway involves an initial two-body fragmentation of HNO_3^{2+} to form $OH^+ + NO_2^+$, followed by further dissociation of these singly charged ions to form $H^+ + NO^+$ accompanied by complete fragmentation of the neutral oxygen atoms [Eq. (11)]:

$$\begin{array}{lccc} HNO_3^{2+} \rightarrow & OH^{+*} & + & NO_2^{+*} \\ & \downarrow & & \downarrow \\ & H^+ & + & NO^+ + 2O \end{array} \qquad (11)$$

The value of $E(HNO_3^{2+})$ associated with this fragmentation pathway [Eq. (11)] is 39.1 eV, a value close to the energy of the dication state we deduced was responsible for the reactions in group 1. Indeed, we deduce all three of these dissociation reactions ($OH^+ + NO^+$, $O^+ + NO^+$, and $H^+ + NO^+$) proceed via the initial fragmentation of HNO_3^{2+} to $OH^+ + NO_2^+$. Therefore, it is possible that the formation of the $OH^+ + NO^+$, $O^+ + NO^+$, and $H^+ + NO^+$ ion pairs is a result of the dissociation of the same dicationic electronic state.

4.4. Group 4: $H^+ + NO_2^+$

The coincidence signals corresponding to the $H^+ + NO_2^+$ peak (Fig. 2) lie between a time-of-flight difference of 2.7 and 2.85 μs. The experimentally determined appearance energy (Table 2) for this dissociation reaction is determined to be 40 $\pm$ 5 eV, a value with a larger uncertainty than can usually be achieved ($\pm$2 eV) because of the extremely weak coincidence signals at low electron energies. Table 1 shows the values of $E(HNO_3^{2+})$ derived assuming the dissociation of HNO_3^{2+} via an initial two-body charge separation and subsequent dissociation of the singly charged ions to form the observed ion pair. From Table 1, the value of $E(HNO_3^{2+})$ derived assuming an initial fragmentation to form $OH^+ + NO_2^+$, 32.2 eV, is clearly outside the error limits of the threshold. This dissociation mechanism is therefore not likely to be followed. The remaining pathway involves an initial charge-separating reaction to form $H^+ + NO_3^+$, the latter ion subsequently dissociating to form the pair observed in the coincidence spectrum [Eq. (12)]:

$$\begin{array}{lccc} HNO_3^{2+} \rightarrow & H^+ & + & NO_3^+ \\ & \downarrow & & \downarrow \\ & H^+ & + & NO_2^+ + O \end{array} \qquad (12)$$

Interpretation of the coincidence peak widths (Table 1) assuming the decay of the dication via this pathway yields a value of $E(HNO_3^{2+})$ of 37.9 eV, an estimate lying within the error limits of the experimentally determined threshold.

5. General discussion

The above conclusions are summarized in Table 4, which lists the dissociation reactions observed, appearance energies and the derived energetic data given the most probable dissociation pathway. The above comparisons of the values of the dication state energy, derived from the coincidence peak widths in the ion–ion coincidence spectrum of HNO_3^{2+} for each dissociation reaction, with the experimentally determined threshold for the four groups of peaks suggests that the fragmentation of the nitric acid dictation involves three initial two-body charge separations. These initial charge separations involve the cleavage of the three different bonds in the dication. The three distinct bond cleavages (Table 4) are the breaking of

Table 4
Proposed decay pathways and estimates of the KER upon dissociation, the energies of the dication electronic states responsible for the observed reactions and their appearance energies, where available. The values for the three-body reactions are obtained assuming the indicated initial two-body charge separation and subsequent dissociation of the monocations accompanied by complete fragmentation of the neutral products

Dissociation reaction	Initial charge separation	KER /eV	$E(HNO_3^{2+})$ /eV	Appearance energy/eV
$OH^+ + NO^+$ [+O]	$OH^+ + NO_2^+$	7.7	35.3	39.0 ± 2
$O^+ + NO^+$ [+H + O]	$OH^+ + NO_2^+$	7.0	39.6	39.0 ± 2
$OH^+ + NO_2^+$	$OH^+ + NO_2^+$	5.8	30.7	—
$O^+ + HNO_2^+$	$O^+ + HNO_2^+$	—	—	—
$H^+ + N^+$ [+3O]	—	—	—	—
$H^+ + O^+$ [+N + 2O]	—	—	—	—
$H^+ + NO^+$ [+2O]	$OH^+ + NO_2^+$	6.5	39.1	40 ± 5
$H^+ + NO_2^+$ [+O]	$H^+ + NO_3^+$	8.0	37.9	40 ± 5

the H—O bond in the molecular dication, which eventually leads to the formation of $H^+ + NO_2^+$, the breaking of one of the O—N bonds resulting in the formation of $O^+ + HNO_2^+$, and the breaking of the HO—N bond forming $OH^+ + NO_2^+$, followed by further dissociation to form $OH^+ + NO^+$, $O^+ + NO^+$, and $H^+ + NO^+$. As described above, it is not possible to determine the fragmentation pathway that leads to the formation of $H^+ + N^+$ and $H^+ + O^+$ because of the lack of information concerning energetics and appearance energies for these ion pairs.

An obvious extension of this work would be to investigate the decay of HNO_3^{2+} by using triple coincidence technology [35]. Such experiments, which will undoubtedly provide further information on the decay pathways of this doubly charged ion, are underway.

6. Conclusion

Ion–ion coincidence experiments have been performed to study the formation and dissociation of HNO_3^{2+}. Coincidence peaks due to the dissociation of HNO_3^{2+} to yield $OH^+ + NO^+$, $O^+ + NO^+$, $OH^+ + NO_2^+$, $O^+ + HNO_2^+$, $H^+ + N^+$, $H^+ + O^+$, $H^+ + NO^+$, and $H^+ + NO_2^+$ ion pairs were observed showing HNO_3^{2+} dissociates via a variety of two- and three-body reactions. Comparisons of experimentally determined threshold values for the four distinct groups of peaks with values of the dication state energy derived from coincidence peak widths for each dissociation reaction are consistent with the model of the initial charge separation as a two-body reaction involving either an O—H, O—N, or HO—N dication bond cleavage. The three-body reactions involve subsequent dissociation of one or more of the primary monocations to produce the detected ion pairs accompanied by complete fragmentation of the neutral products.

The values derived for the energies of the dication state responsible for forming the $OH^+ + NO^+$, $O^+ + NO^+$, and $H^+ + NO^+$ indicate that these dissociation reactions may all occur from the same electronic state of the dication.

The energy of the dication state responsible for the two-body dissociation reaction $OH^+ + NO_2^+$ indicates that this dissociation reaction occurs from the ground electronic state of HNO_3^{2+}, thus providing a first estimate of the double ionization energy of HNO_3^{2+} as 30.7 ± 0.2 eV.

Acknowledgements

We would like to acknowledge the Nuffield Foundation, the Central Research Fund of the University of London, and the UCL Graduate School for equipment grants and the EPSRC for the award of a Research Studentship to CSSO'C.

References

[1] B.A. Thrush, Rep. Prog. Phys. 51 (1988) 1341.
[2] M. Suto, L.C. Lee, J. Chem. Phys. 81 (1984) 1294.
[3] R.A. Friedel, J.L. Shultz, A.G. Sharkey, Anal. Chem. 1 (1959) 1128.
[4] H.-W. Jochims, W. Denzer, H. Baumgärtel, O. Lösking, H. Willner, Ber. Bunsenges. Phys. Chem. 96 (1992) 573.
[5] C.S.S. O'Connor, N.C. Jones, S.D. Price, Int. J. Mass Spectrom. Ion. Proc. 163 (1997) 131.
[6] M. Larsson, Comments At. Mol. Phys. 29 (1993) 39.
[7] D. Mathur, Phys. Rep. 225 (1993) 193.
[8] S.D. Price, J. Chem. Soc. Faraday Trans. 93 (1997) 2451.
[9] D. Mathur, L.H. Andersen, P. Hvelplund, D. Kella, C.P. Safvan, J. Phys. B: At. Mol. Opt. Phys. 28 (1995) 3415.
[10] L.H. Andersen, J.H. Posthumus, O. Vahtras, H. Agren, N. Elander, A. Nunez, A. Scrinzi, M. Natiello, M. Larsson, Phys. Rev. Lett. 71 (1993) 1812.
[11] J. Senekowitsch, S. O'Neil, P. Knowles, H.J. Werner, J. Phys. Chem. 95 (1991) 2125.
[12] G. Dawber, A.G. McConkey, L. Avaldi, M.A. Macdonald, G.C. King, R.I. Hall, J. Phys. B: At. Mol. Opt. Phys. 27 (1994) 2191.
[13] P. Lablanquie, M. Lavollee, J.H.D. Eland, F. Penent, R.I. Hall, Meas. Sci. Technol. 6 (1995) 939.
[14] M. Lundqvist, P. Baltzer, D. Edvardsson, L. Karlsson, B. Wannberg, Phys. Rev. Lett. 75 (1995) 1058.
[15] D.M. Szaflarski, A.S. Mullin, K. Yokoyama, M.N.R. Ashfold, W.C. Lineberger, J. Phys. Chem. 95 (1991) 2122.
[16] D.M. Curtis, J.H.D. Eland, Int. J. Mass Spectrom. Ion. Proc. 63 (1985) 241.
[17] W.C. Wiley, I.H. McLaren, Rev. Sci. Instrum. 26 (1955) 1150.
[18] K.A. Newson, S.D. Price, Int. J. Mass Spectrom. Ion. Proc. 153 (1996) 151.
[19] C.S.S. O'Connor, N.C. Jones, S.D. Price, Chem. Phys. 214 (1997) 131.
[20] K.E. McCulloh, T.E. Sharp, H.M. Rosenstock, J. Chem. Phys. 42 (1965) 3501.
[21] G. Dujardin, S. Leach, O. Dutuit, P.M. Guyon, M. Richard-viard, Chem. Phys. 88 (1984) 339.
[22] T. Masuoka, Phys. Rev. A 48 (1993) 1955.
[23] K.A. Newson, S.M. Luc, S.D. Price, N.J. Mason, Int. J. Mass Spectrom. Ion. Proc. 148 (1995) 203.
[24] P.G. Fournier, J.H.D. Eland, P. Millie, S. Svensson, S.D. Price, J. Fournier, G. Comtet, B. Wannberg, L. Karlsson, P. Baltzer, A. Kaddouri, U. Gelius, J. Chem. Phys. 89 (1988) 3553.
[25] L.J. Frasinski, M. Stankiewicz, P.A. Hatherly, K. Codling, Meas. Sci. Technol. 3 (1992) 1188.
[26] C.S.S. O'Connor, N. Tafadar, S.D. Price, J. Chem. Soc. Faraday Trans. 94 (1998) 1797.
[27] J.H.D. Eland, Mol. Phys. 61 (1987) 725.
[28] S. Hsieh, J.H.D. Eland, J. Chem. Phys. 103 (1995) 1006.
[29] I. Nenner, J.H.D. Eland, Z. Phys. D, 25 (1992) 47.
[30] J.H.D. Eland, Chem. Phys. Lett. 203 (1993) 353.
[31] K. Codling, L.J. Frasinski, P.A. Hatherly, M. Stankiewicz, F.P. Larkins, J. Phys. B: At. Mol. Opt. Phys., 24 (1991) 951.
[32] M. Simon, P. Morin, P. Lablanquie, M. Lavollee, K. Ueda, N. Kosugi, Chem. Phys. Lett. 238 (1995) 42.
[33] S.G. Lias, J.E. Bartmess, J.F. Liebman, J.L. Holmes, R.D. Levin, W.G. Mallard, J. Phys. Chem. Ref. Data 17 S1 (1988) 1.
[34] B.P. Tsai, J.H.D. Eland, Int. J. Mass Spectrom. Int. Proc. 36 (1980) 143.
[35] J.H.D. Eland, F.S. Wort, R.N. Royds, J. Electron Spectrosc. Relat. Phenom. 41 (1986) 297.